Eur Spine J (2004) 13 : 61–68
DOI 10.1007/s00586-003-0590-3

ORIGINAL ARTICLE

P. C. Ivancic
A. M. Pearson
M. M. Panjabi
S. Ito

Injury of the anterior longitudinal ligament during whiplash simulation

Received: 20 December 2002
Revised: 17 March 2003
Accepted: 20 June 2003
Published online: 14 November 2003

This research was supported by NIH Grant 1 R01 AR45452 1A2 and the Doris Duke Charitable Foundation

P. C. Ivancic · A. M. Pearson
M. M. Panjabi (✉) · S. Ito
Biomechanics Research Laboratory,
Department of Orthopaedics
and Rehabilitation,
Yale University School of Medicine,
333 Cedar St., P.O. Box 208071,
New Haven, CT 06520-8071, USA
Tel.: +1-203-7852812,
Fax: +1-203-7857069,
e-mail: manohar.panjabi@yale.edu

Abstract Anterior longitudinal ligament (ALL) injuries following whiplash have been documented both in vivo and in vitro; however, ALL strains during the whiplash trauma remain unknown. A new in vitro whiplash model and a bench-top trauma sled were used in an incremental trauma protocol to simulate whiplash at 3.5, 5, 6.5 and 8 g accelerations, and peak ALL strains were determined for each trauma. Following the final trauma, the ALLs were inspected and classified as uninjured, partially injured or completely injured. Peak strain, peak intervertebral extension and increases in flexibility parameters were compared among the three injury classification groups. Peak ALL strains were largest in the lower cervical spine, and increased with impact acceleration, reaching a maximum of 29.3% at C6-C7 at 8 g. Significant increases ($P<0.05$) over the physiological strain limits first occurred at C4-C5 during the 3.5 g trauma and spread to lower intervertebral levels as impact severity increased. The complete ligament injuries were associated with greater increases in ALL strain, intervertebral extension, and flexibility parameters than were observed at uninjured intervertebral levels ($P<0.05$).

Keywords Spine biomechanics · Anterior longitudinal ligament · Whiplash · Injury mechanism · Spinal instability

Introduction

Whiplash trauma has been linked to chronic neck pain, though the pathophysiology underlying Whiplash-Associated Disorders remains unknown [37, 40, 42]. Approximately 50% of whiplash patients have reported chronic neck pain 15 years after the trauma [3, 41]. Various anatomical structures have been identified as potential injury sites, with many recent investigations focusing on the facet joint [1, 7, 19, 21]. In vivo and in vitro studies have shown that the lower cervical spine hyperextends during the initial phase of whiplash [12, 18]. While hyperextension may cause facet joint compression injuries, it may also result in excessive strains in the anterior soft tissues [32].

There is significant clinical and biomechanical evidence demonstrating that anterior longitudinal ligament (ALL) and anterior annulus injuries often occur simultaneously during whiplash. A magnetic resonance imaging study demonstrated injuries to both components in whiplash patients, and similar injuries have also been discovered at surgery and autopsy [4, 8, 16]. Whiplash simulations using cadavers and monkeys have also produced ALL tears and anterior disc detachments [22, 46]. Similar injuries commonly occurred in the lower cervical spine due to hyperextension loading of a whole cervical spine (WCS) model [39].

Clinical and biomechanical studies have also demonstrated that soft tissue injuries of the cervical spine can lead to instability. Subacute instability of the cervical spine has been reported in patients presenting with neck pain and normal radiographs, who subsequently developed clinical instability, most likely due to ligamentous injury [14]. In vitro investigations have demonstrated that transection or

injury of the ALL and anterior annulus resulted in increased flexibility under extension loading, implying that injury to these components could lead to instability [25, 27, 38]. This composite evidence suggests that ALL and anterior annulus injury may lead to clinical instability and pain [26].

Strains and injury patterns of the anterior soft tissues of the cervical spine during whiplash are unknown. Simulation of whiplash trauma using a WCS model is effective in quantifying soft tissue injury [31, 33]. The goals of this investigation were:

1. To quantify ALL strains during simulated whiplash at various trauma energies using a whole cervical spine model with muscle force replication
2. To document partial and complete ALL injuries macroscopically
3. To determine whether ALL strain increases were associated with injuries, and
4. To evaluate the relationship between the ALL injuries and spinal instability

Materials and methods

Specimen preparation

Six fresh-frozen human osteoligamentous WCS specimens (four male, two female, average age 70.8 years, range 52–84 years) were mounted in resin (Fiberglass Evercoat, Cincinatti, OH) at the occiput and T1 according to a pre-defined neutral posture, such that a line from the top of the dens to the lowest point on the posterior occiput was parallel to the occipital mount, and the T1 vertebra was tilted anteriorly by 24° [2]. To attach the lightweight motion-tracking flags, a headless wood screw was drilled into the anterior aspect of each vertebra (C1–C7). The flags consisted of 3-mm-diameter hollow brass tubes with two white, spherical, radio-opaque markers (Fig. 1). A flag was fitted rigidly onto each wood screw, and additional flags were attached to the occipital and T1 mounts. This constituted the WCS model.

To prepare a specimen for whiplash trauma, a surrogate head (mass 3.3 kg and sagittal plane moment of inertia 0.016 kg.m^2) was attached to the occipital mount of the WCS model, and its center of gravity was located in anatomic position with respect to the spine specimen. The surrogate head and spine were stabilized using the compressive muscle force replication (MFR) system (Fig. 2) [15]. The MFR system consisted of four anterior, two posterior and eight lateral cables attached to preloaded springs anchored to the base. The stiffness coefficient of each spring was 4.0 N/mm. The anterior cables ran through guideposts at C4 (two cables per post), through pulleys within the T1 mount, and finally were connected to two springs (two cables per spring). The preload in each anterior spring was 15 N. Two posterior MFR cables were connected to the occipital mount and ran through wire loops attached to the spinous processes of each vertebra (C2–C7), through a pulley within the T1 mount and to a spring preloaded at 30 N. Bilateral MFR cables originated from C0, C2, C4 and C6, passed alternately along lateral guide rods, ran through pulleys at the T1 mount and were attached to the springs preloaded at 30 N. With this MFR arrangement the compressive preloads at each intervertebral level were: 120 N (C0-C1, C1-C2); 180 N (C2-C3, C3-C4); 240 N (C4-C5, C5-C6); and 300 N (C6-C7, C7-T1). The MFR system fully supported the head such that no counterweight was needed to suspend the head in the neutral posture. A C0–C2 flexion limiter was used to simulate the effect of contact between the chin and the anterior

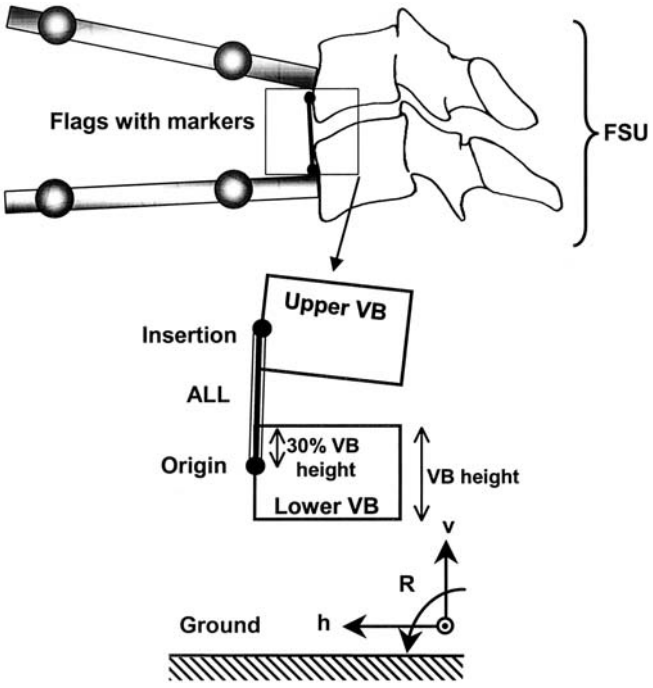

Fig. 1 Schematic of functional spinal unit (FSU), as seen on a lateral radiograph, showing the motion-tracking flags on the upper and lower vertebral bodies (VBs) of the FSU and the anterior longitudinal ligament (ALL). *ALL Origin* represents the inferior end of the ALL located at 30% of the lower VB height inferior to the anterosuperior corner of the lower VB along its anterior edge [28, 29] and *ALL Insertion* represents the superior end of the ALL located at 30% of the upper VB height superior to the anteroinferior corner of the upper VB along its anterior edge [28, 29]. The ground coordinate system (h-v) was fixed to the ground throughout the trauma. Rotation (R) was defined with flexion positive and extension negative

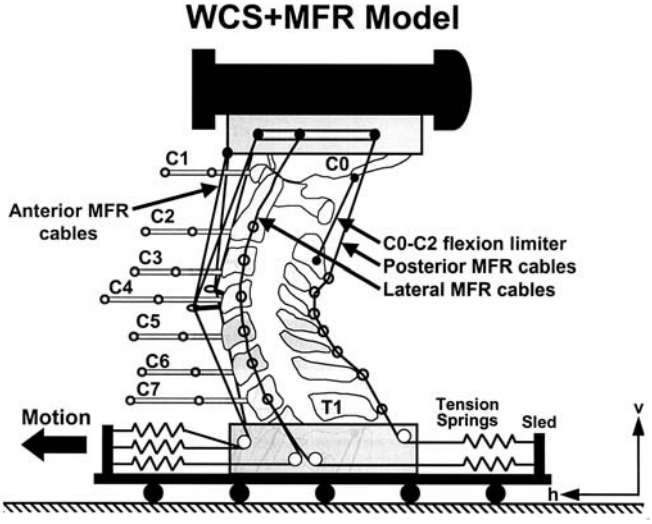

Fig. 2 The biofidelic whole cervical spine model with muscle force replication (WCS+MFR). Anterior, posterior and bilateral MFR cables stabilized the head during simulated whiplash. The C0–C2 flexion limiter restricted upper cervical spine flexion to within physiological limits. For additional details, please see the text

cervical structures (i.e., skin, subcutaneous fat, strap muscles, sternum) on flexion of C0-C1 and C1-C2 [34]. It consisted of a nylon-coated steel cable (180 N load capacity, 0.6 mm diameter, part no. Y-MCX-24, Small Parts, Inc., Miami Lakes, FL) secured to the occipital mount and to the C2 spinous process, and allowed approximately 30° of sagittal rotation, consistent with the in vivo data of the normal cervical spine [10, 20, 24]. This constituted the WCS+MFR model.

Flexibility testing

Sagittal flexibility testing was performed on the WCS model when intact and following the 8 g trauma to determine the neutral zone (NZ) and range of motion (ROM) at each intervertebral level [30]. Pure flexion and extension moments up to a maximum of 1.5 Nm were applied to the occipital mount in four equal steps. To minimize viscoelastic effects, 30-s wait periods were given following each load application. Data were collected on the third loading cycle, following two pre-conditioning cycles.

Trauma production and monitoring

Rear-impact whiplash simulation was performed using a previously developed bench-top sled apparatus [15, 31]. An incremental trauma protocol was used to rear-impact the WCS+MFR model at 3.5, 5, 6.5 and 8 g, following the initial 2 g dynamic pre-conditioning that was necessary due to the viscoelastic behavior of the soft tissues [26]. High-speed digital cameras (Fastcam, Super 10 K, model PS-110, Eastman Kodak Co, Rochester, NY) recorded the spinal motions at 500 f/s.

Anterior longitudinal ligament construction and tracking during trauma

A lateral radiograph of the WCS model in the neutral posture was taken and digitally scanned (Adobe Photoshop version 6.01, San Jose, CA). The heights of the vertebral bodies (VBs) were determined, and the ALL origins and insertions were selected based on the quantitative anatomy of the cervical vertebrae and ligaments (Fig. 1) [28, 29]. To define geometrical rigid body relationships between the centers of the flag markers and the ALL insertion and origin for each vertebra, these points were digitized in the ground coordinate system h-v. The geometrical rigid body relationships established on the radiograph were used to superimpose the ALL origins and insertions onto the first frame of the high-speed movie. Custom motion-tracking software written in Matlab (The Mathworks Inc., Natick, MA) automatically calculated the intervertebral rotations and the flag marker translations at each subsequent frame. These data, together with the geometrical rigid body relationships, were used to calculate the translation of each ALL origin and insertion in the ground coordinate system during trauma. The strain within each mathematically reconstructed ALL was calculated by dividing the increase in ALL length by the original ALL length (expressed in percent). The average error in the computation of ALL elongation was 0.3 mm (SD 0.2 mm), which corresponded to an average strain error of 2.3% (SD 1.5%) [35].

Injury documentation

Following the 8 g trauma, each ALL was visually inspected and classified as belonging to one of the three injury classes: no macroscopic injury (class 0), partial injury with no visible damage to the underlying annulus (class I), or complete injury with anterior annulus involvement (class II) [25]. While the ALL can blend laterally with connective tissue and posteriorly with the anterior annu-

Table 1 Average (SD) neutral anterior longitudinal ligament (ALL) lengths (mm) and peak ALL elongations (mm) and strains (%) during physiological extension and simulated whiplash. *P*-values are given for differences between peak trauma strain and the corresponding physiological strain; $P<0.05$ indicates a significant difference, $P<0.1$ indicates a trend

Level	Neutral ALL length (mm)	Physiological extension		3.5 g Trauma		5 g Trauma		6.5 g Trauma		8 g Trauma	
		Elongation (mm)	Strain (%)	Elongation (mm)	Strain (%)	Elongation (mm)	Strain (%)	Elongation (mm)	Strain (%)	Elongation (mm)	Strain (%)
C2-C3	13.3 (1.3)	0.5 (0.6)	4.1 (4.6)	1.8 (0.9)	13.5 (6.8)	2.0 (1.4)	14.9 (10.4)	2.0 (1.5)	15.4 (11.2)	2.0 (1.3)	15.4 (9.8)
C3-C4	14.5 (2.4)	0.9 (0.4)	6.5 (3.0)	0.9 (0.5)	6.2 (3.3)	1.8 (1.2)	12.7 (8.6)	3.4 (2.5)	23.7 (17.1)	3.6 (2.4)	25.0 (16.6)**
C4-C5	13.5 (2.1)	0.8 (0.6)	6.2 (4.4)	2.8 (1.8)	20.8 (13.6)*	3.4 (1.6)	25.3 (12.1)*	3.7 (1.6)	27.5 (11.8)*	3.7 (1.5)	27.7 (11.0)*
C5-C6	11.6 (2.8)	1.8 (1.1)	15.1 (9.8)	2.3 (1.5)	20.0 (13.1)	3.3 (1.1)	28.3 (9.3)*	3.0 (1.7)	26.0 (14.3)**	3.4 (2.4)	29.0 (20.6)*
C6-C7	13.5 (2.2)	1.4 (1.0)	10.6 (7.4)	2.7 (2.6)	19.8 (19.1)	2.9 (2.0)	21.5 (15.1)	3.6 (2.6)	26.7 (19.1)*	4.0 (3.0)	29.3 (22.0)*

* $P<0.05$; ** $P<0.1$

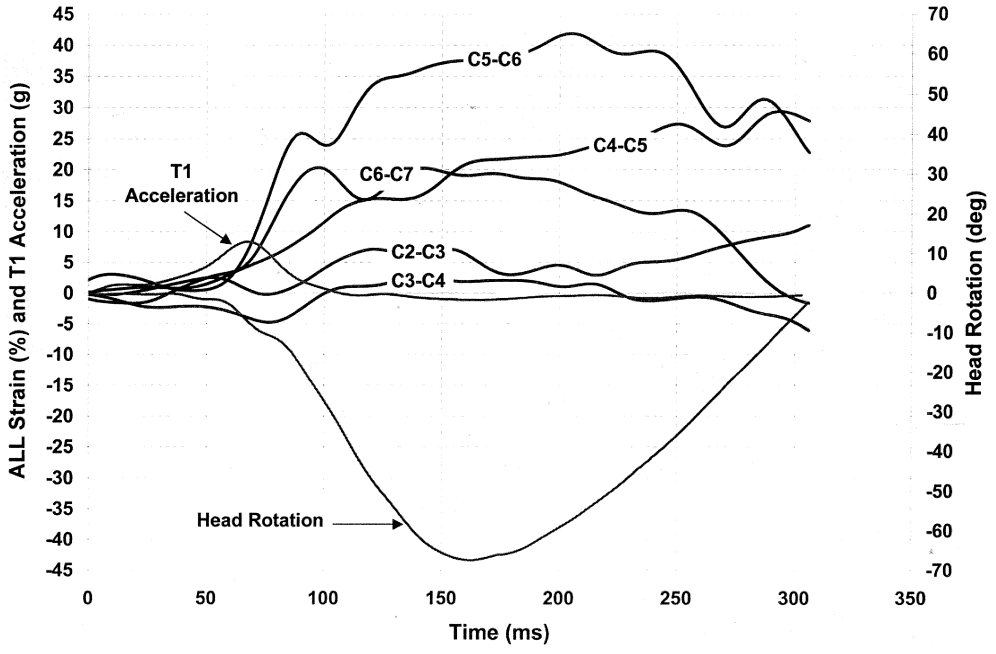

Fig. 3 Anterior longitudinal ligament (ALL) strains at various spinal levels (C2-C3 to C6-C7) during simulated whiplash (specimen 3, 8 g trauma). Sled (T1) acceleration and head rotation are also shown

lus, two independent investigators had perfect interobserver agreement in the evaluation of the injuries.

Data analysis

The ALL strain data were low-pass digitally filtered at a cut-off frequency of 30 Hz, and the peak strains during each trauma were identified. Residual and Fourier analysis demonstrated that most of the signal power was contained under 20 Hz. Physiological ALL strains were measured during flexibility testing of the intact WCS models subjected to a 1.5-Nm extension moment using the ALL tracking method described above. The application of a 1.5-Nm pure extension moment resulted in intervertebral rotations that were within the physiological range [24, 36, 43], and thus provided physiological ALL strains. Statistical differences between peak trauma and corresponding physiological ALL strains were determined using single-factor, repeated measures ANOVA and Bonferroni post-hoc tests (Minitab Rel. 13, State College, PA). Comparisons among the three ALL injury classes were performed to determine increases in the trauma parameters (ALL strain and intervertebral extension) and the flexibility parameters [neutral zone (NZ) and range of motion (ROM)]. The ALL strain and intervertebral extension increases were defined as the peak trauma value minus the physiological value (determined during intact flexibility testing). The NZ and ROM increases were defined as the post-8 g value minus the intact value. Comparisons were made using ANOVA and Bonferroni pairwise post-hoc tests. Significance was set at $P<0.05$, with a trend towards significance defined at $P<0.1$.

Results

The average overall ALL length was 13.3 mm and ranged from 11.6 mm at C5-C6 to 14.5 mm at C3-C4 (Table 1). These lengths compared favorably with the average overall ALL length of 13.1 mm measured in a previous in vitro study [29]. The ALL kinematics varied among specimens and intervertebral levels, though a typical pattern was observed (Fig. 3: specimen 3, 8 g trauma). The ALL tended to elongate as the head extended and then returned towards its original length as the head returned to the neutral position. Significant increases ($P<0.05$) in the ALL strains in excess of the corresponding physiological strains were first observed at C4-C5 during the 3.5 g trauma and then spread to C5-C6 at 5 g and C6-C7 at 6.5 g (Fig. 4). A trend towards an increase in ALL strain over the corresponding physiological value was detected at C3-C4 at 8 g ($P=0.078$). The peak ALL strains were largest in the lower cervical spine and increased with impact acceleration, with an average peak strain of 29.3% (corresponding to an average elongation of 4.0 mm) observed at C6-C7 during the 8 g trauma (Table 1).

Following the final trauma, macroscopic ALL injuries were observed in the middle and lower cervical spine (C3-C7) (Fig. 5). Of the 30 ALLs evaluated, 4 sustained class I injuries (1 at C3-C4, 2 at C4-C5 and 1 at C6-C7), 6 sustained class II injuries (3 at C3-C4, 2 at C5-C6, and 1 at C6-C7), and 20 were uninjured (class 0). Note that the specimens in class 0 could have sustained injuries that were not visible grossly. Comparison of the class II and class 0 trauma parameters increases (ALL strain and intervertebral extension) showed that both were significantly greater ($P<0.05$) in class II (Table 2). The average class II ALL strain increase (39.2%) was more than double the average class 0 increase (17.5%). Comparing class I and class II, there were no significant differences, though there was a trend towards a greater increase in ALL strain in class II ($P=0.054$).

The increases in NZ and ROM were greater in class II than class 0 (Table 2). The class II NZ increase (8.7°) was more than 250% of the Class 0 NZ increase, and the class II

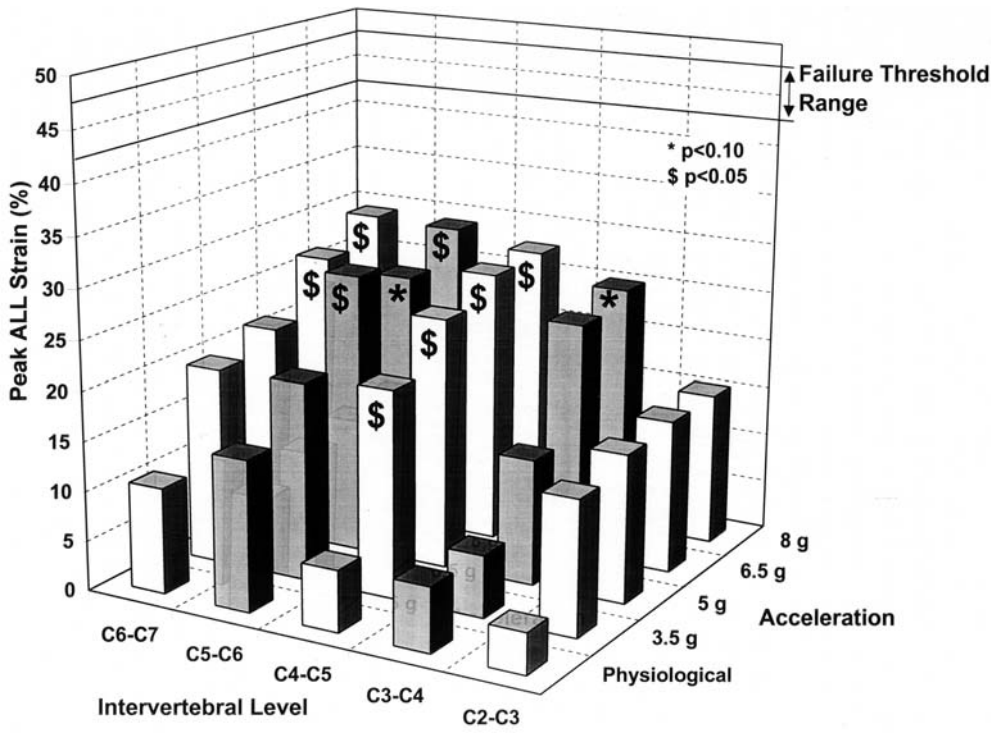

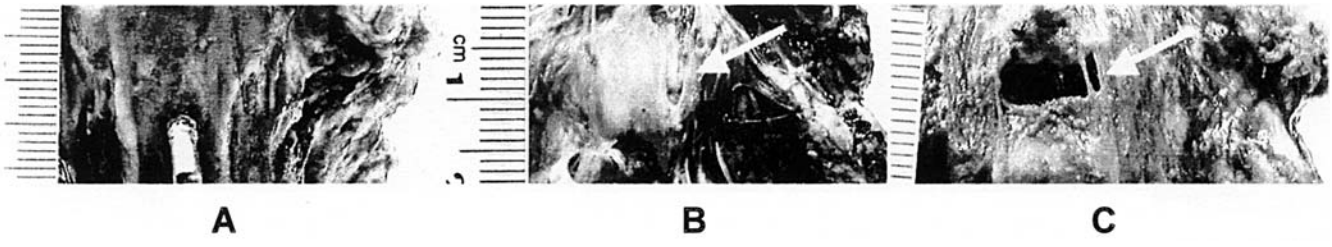

Fig. 4 Average peak ALL strains at C2-C3 to C6-C7 during physiological loading and simulated whiplash (3.5 g to 8.0 g). The failure threshold range was adapted from Yoganandan et al. 2000 [45]

Fig. 5 Examples of the three ALL injury classes. **A** Class 0: macroscopically uninjured ALL (C6-C7). **B** Class I: partial ALL injury without involvement of the underlying annulus (C3-C4). **C** Class II: complete ALL injury with injury to underlying disc (C5-C6)

ROM increase (8.5°) was more than 350% of the class 0 ROM increase. Comparing class I and class II, there were no significant differences, though there was a trend towards a greater increase in ROM in class II (P=0.06). While mean values for trauma and flexibility parameters were greater for class I than class 0, these differences failed to reach significance.

Discussion

Anterior longitudinal ligament (ALL) and anterior annulus injuries have been documented following whiplash trauma [4, 8]; however, no studies have evaluated the ALL injury mechanism during simulated whiplash. The results of the current study demonstrated that the greatest ALL strains occurred in the lower cervical spine and that ALL strains increased with impact severity. Increases over the physiological strains were observed in the middle and lower cervical spine (C3–C7) at trauma energies of 3.5 g and above, suggesting that the ALLs spanning these levels were at the greatest risk for injury.

Analysis of the class 0 (no macroscopic ALL injury), class I (partial ALL injury), and class II (complete ALL injury with underlying anterior annulus damage) injury categories demonstrated greater increases in ALL strain and intervertebral extension in class II than in class 0. This suggests that greater intervertebral extension is associated with greater ALL strain and higher injury potential. Class II injuries also resulted in greater increases in the neutral zone (NZ) and range of motion (ROM) as compared to class 0, demonstrating that severe injuries led to measurable instability. While mean class I trauma and flexibility parameter increases were greater than class 0, significance was not obtained (P>0.05), possibly due to the small class I sample size (n=4). The results suggest, however, that increased intervertebral extension resulted in higher ALL

Table 2 Average (SD) increases in trauma and flexibility parameters

Injury class	*n*	Trauma parameters		Flexibility parameters	
		ALL strain (%)	Intervertebral extension (deg)	NZ (deg)	ROM (deg)
Class 0	20	17.5 (11.0)	4.4 (3.4)	3.2 (2.6)	2.2 (1.9)
Class I	4	22.2 (9.1)	7.1 (5.0)	4.5 (2.1)	3.0 (1.6)
Class II	6	39.2 (8.9)*	11.4 (8.7)*	8.7 (5.1)*	8.5 (7.1)*

* $P<0.05$ (Significant differences between class II and class 0)

strains and that such increases were associated with the progression of injury and development of instability.

The limitations of the current whole cervical spine model with muscle force replication (WCS+MFR) must be considered when formulating conclusions regarding clinically relevant injury mechanisms. These limitations, including the fixation of T1 to the trauma sled and lack of active muscle force simulation, have been addressed previously [6, 31, 32, 33]. The calculation of ALL strains was based on the assumption that the vertebra and its motion-tracking flag constituted a rigid body. During whiplash trauma, it is unlikely that vertebral deformation was of a sufficient magnitude to significantly alter the results. In addition, the ALLs analyzed in this study were mathematically reconstructed based on in vitro measurements of the quantitative anatomy of the cervical spine [29]. As such, the ALL strains reported in this study represent approximations of the actual strains based on the mathematical representations of the ligaments. Despite these limitations, we believe our results are biomechanically and clinically relevant.

The injuries documented in the current study compare favorably to those observed clinically and those found in other whiplash simulations. Davis et al. reported ALL tears with underlying anterior annulus damage at C5-C6 and C6-C7 in two of nine whiplash patients imaged with MRI [8]. In a series of ten patients who underwent cervical intervertebral fusion for instability following whiplash, five were reported to have ALL and anterior disc injuries [4]. A previous whiplash simulation using whole cadavers at impact accelerations up to 4.5 g documented ALL injuries in the lower cervical spine in three of four cadavers [46]. The current study has demonstrated similar injuries, with complete and partial ALL tears observed in the mid and lower cervical spine (C3–C7). While the injuries observed in the earlier whiplash simulation [46] were limited to the lower cervical spine, the higher final impact acceleration of 8 g in the current study likely resulted in the spread of injuries to the mid cervical spine as well.

No data exist for direct comparison of the ALL strains observed during the current whiplash simulation; however, failure strains for cervical ALLs are available [45]. Though these failure thresholds were determined using static loading, it has been shown that ALL deformation at failure did not vary with the loading rate [44]. Recalculating these ALL failure strains using the ALL lengths in the current study yielded an ALL failure threshold range of 42.6–47.6% [45]. The average peak ALL strains in the current study were under 30%, and thus below the failure threshold. Nonetheless, strains in individual ligaments did exceed the failure threshold, with the class II average peak strain being 48.8%. These data suggest that a minority of the population is at risk for complete ALL tears during whiplash.

The current study and others have shown that injury to the anterior column results in cervical instability, particularly during intervertebral extension [25, 27, 38]. Spinal instability has been suggested to cause pain through a variety of mechanisms including compression of neural structures, increased loading of ligaments innervated with mechanoreceptors, and muscle fatigue resulting from an increased reliance on spinal musculature to provide stability [26]. While data on spinal ligament healing is limited, it has been shown that annular lesions heal poorly [13, 17]. If ALL and anterior annulus injuries do not completely heal, clinical instability and chronic pain could develop. It is likely that some patients with chronic neck pain following whiplash trauma suffer from cervical instability as a result of mechanical disruption of the anterior stabilizing system.

Injury to the passive anterior column soft tissues could also result in increased loading and degeneration of the posterior spinal components. Studies of the lumbar spine using animal models have shown that injury to the anterior annulus is followed by fibrosis of the nucleus pulposus and osteoarthritic changes in the facet joints [13, 17, 23]. A biomechanical investigation demonstrated that a decrease in disc height resulted in increased loading of the lumbar facet joint [9]. Clinical support for the hypothesis that disc degeneration leads to facet osteoarthritis is found in radiographic studies that demonstrated lumbar facet joint osteoarthritis rarely occurred without prior disc degeneration [5, 11]. Although the lumbar and cervical spine are exposed to different compressive loads and have different facet joint anatomy, ALL and anterior annulus injuries sustained in whiplash could hypothetically lead to increased loading, pain and osteoarthritis of the cervical facet joints. This process may contribute to the chronic facet joint pain that has been documented in some whiplash patients [21].

Conclusions

The current study has shown that ALL strains during simulated whiplash were greatest in the lower cervical spine,

and, on average, below the ALL failure threshold. Select ALLs did fail during the simulated whiplash trauma, and these ligaments had undergone higher strains than the uninjured ligaments. The intervertebral levels associated with complete ALL injuries were shown to have greater increases in NZ and ROM than uninjured levels, implying that these injuries produced spinal instability. In patients with similar injuries, incomplete healing could lead to clinical instability and long-term pain. As disc degeneration results in increased facet loading, anterior column injury sustained during whiplash could lead to chronic facet pain. It is our hope that the current results can help guide future investigations of the long-term symptoms associated with whiplash injury.

References

1. Barnsley L, Lord S, Bogduk N (1994) Whiplash injury. Pain 58:283–307
2. Braakman R, Penning L (1971) Injuries of the cervical spine. Excerpta Medica, Amsterdam
3. Bunketorp L, Nordholm L, Carlsson J (2002) A descriptive analysis of disorders in patients 17 years following motor vehicle accidents. Eur Spine J 11: 227–234
4. Buonocore E, Hartman JT, Nelson CL (1966) Cineradiograms of cervical spine in diagnosis of soft-tissue injuries. JAMA 198:143–147
5. Butler D, Trafimow JH, Andersson GB, McNeill TW, Huckman MS (1990) Discs degenerate before facets. Spine 15:111–113
6. Cholewicki J, Panjabi MM, Nibu K, et al (1998) Head kinematics during in vitro whiplash simulation. Accid Anal Prev 30:469–479
7. Cusick JF, Pintar FA, Yoganandan N (2001) Whiplash syndrome: kinematic factors influencing pain patterns. Spine 26:1252–1258
8. Davis SJ, Teresi LM, Bradley WG Jr, Ziemba MA, Bloze AE (1991) Cervical spine hyperextension injuries: MR findings. Radiology 180:245–251
9. Dunlop RB, Adams MA, Hutton WC (1984) Disc space narrowing and the lumbar facet joints. J Bone Joint Surg Br 66:706–710
10. Dvorak J, Panjabi MM, Novotny JE, Antinnes JA (1991) In vivo flexion/extension of the normal cervical spine. J Orthop Res 9:828–834
11. Fujiwara A, Tamai K, Yamato M, et al (1999) The relationship between facet joint osteoarthritis and disc degeneration of the lumbar spine: an MRI study. Eur Spine J 8:396–401
12. Grauer JN, Panjabi MM, Cholewicki J, Nibu K, Dvorak J (1997) Whiplash produces an S-shaped curvature of the neck with hyperextension at lower levels. Spine 22:2489–2494
13. Hampton D, Laros G, McCarron R, Franks D (1989) Healing potential of the anulus fibrosus. Spine 14:398–401
14. Herkowitz HN, Rothman RH (1984) Subacute instability of the cervical spine. Spine 9:348–357
15. Ivancic PC, Panjabi M, Ito S, Cripton PA, Wang JL (2002) A biofidelic osteoligamentous cervical spine model with muscle force replication for whiplash trauma simulation. Proceedings of the Cervical Spine Research Society. Miami, December 5–7
16. Jonsson H Jr, Bring G, Rauschning W, Sahlstedt B (1991) Hidden cervical spine injuries in traffic accident victims with skull fractures. J Spinal Disord 4: 251–263
17. Kaapa E, Han X, Holm S, et al (1995) Collagen synthesis and types I, III, IV, and VI collagens in an animal model of disc degeneration. Spine 20:59–66
18. Kaneoka K, Ono K, Inami S, Yokoi N, Hayashi K (1997) Human cervical spine kinematics during whiplash loading. International Conference on New Frontiers in Biomechanical Engineering. Tokyo, Japan
19. Kaneoka K, Ono K, Inami S, Hayashi K (1999) Motion analysis of cervical vertebrae during whiplash loading. Spine 24:763–769
20. Lind B, Sihlbom H, Nordwall A, Malchau H (1989) Normal range of motion of the cervical spine. Arch Phys Med Rehabil 70:692–695
21. Lord SM, Barnsley L, Wallis BJ, Bogduk N (1996) Chronic cervical zygapophysial joint pain after whiplash. A placebo-controlled prevalence study. Spine 21:1737–1744
22. MacNab I (1964) Acceleration injuries of the cervical spine. J Bone Joint Surg Am 46:1797–1799
23. Moore RJ, Crotti TN, Osti OL, Fraser RD, Vernon-Roberts B (1999) Osteoarthrosis of the facet joints resulting from anular rim lesions in sheep lumbar discs. Spine 24:519–525
24. Ordway NR, Seymour RJ, Donelson RG, Hojnowski LS, Edwards WT (1999) Cervical flexion, extension, protrusion, and retraction. A radiographic segmental analysis. Spine 24:240–247
25. Oxland TR, Panjabi MM, Southern EP, Duranceau JS (1991) An anatomic basis for spinal instability: a porcine trauma model. J Orthop Res 9:452–462
26. Panjabi MM (1992) The stabilizing system of the spine. II. Neutral zone and instability hypothesis. J Spinal Disord 5:390–396
27. Panjabi MM, White AA 3rd, Johnson RM (1975) Cervical spine mechanics as a function of transection of components. J Biomech 8:327–336
28. Panjabi MM, Duranceau J, Goel V, Oxland T, Takata K (1991) Cervical human vertebrae. Quantitative three-dimensional anatomy of the middle and lower regions. Spine 16:861–869
29. Panjabi MM, Oxland TR, Parks EH (1991) Quantitative anatomy of cervical spine ligaments. II. Middle and lower cervical spine. J Spinal Disord 4: 277–285
30. Panjabi MM, Oxland TR, Lin RM, McGowen TW (1994) Thoracolumbar burst fracture. A biomechanical investigation of its multidirectional flexibility. Spine 19:578–585
31. Panjabi MM, Cholewicki J, Nibu K, Babat LB, Dvorak J (1998) Simulation of whiplash trauma using whole cervical spine specimens. Spine 23:17–24
32. Panjabi MM, Cholewicki J, Nibu K, et al (1998) Mechanism of whiplash injury. Clin Biomech 13:239–249
33. Panjabi MM, Nibu K, Cholewicki J (1998) Whiplash injuries and the potential for mechanical instability. Eur Spine J 7:484–492
34. Panjabi MM, Miura T, Cripton PA, et al (2001) Development of a system for in vitro neck muscle force replication in whole cervical spine experiments. Spine 26:2214–2219
35. Pearson AM, Ivancic PC, Ito S, Panjabi MM (2003) Facet joint kinematics and injury mechanisms during simulated whiplash. Spine (in press)
36. Penning L (1978) Normal movements of the cervical spine. AJR 130:317–326

37. Richter M, Otte D, Pohlemann T, Krettek C, Blauth M (2000) Whiplash-type neck distortion in restrained car drivers: frequency, causes and long-term results. Eur Spine J 9:109–117
38. Richter M, Wilke HJ, Kluger P, Claes L, Puhl W (2000) Load-displacement properties of the normal and injured lower cervical spine in vitro. Eur Spine J 9:104–108
39. Shea M, Wittenberg RH, Edwards WT, White AA 3rd, Hayes WC (1992) In vitro hyperextension injuries in the human cadaveric cervical spine. J Orthop Res 10:911–916
40. Spitzer WO, Skovron ML, Salmi LR, et al (1995) Scientific monograph of the Quebec Task Force on Whiplash-Associated Disorders: redefining "whiplash" and its management. Spine 20:1S–73S
41. Squires B, Gargan MF, Bannister GC (1996) Soft-tissue injuries of the cervical spine: 15-year follow-up. J Bone Joint Surg Br 78:955–957
42. Sturzenegger M, Radanov BP, Di Stefano G (1995) The effect of accident mechanisms and initial findings on the long-term course of whiplash injury. J Neurol 242:443–449
43. White AA 3rd, Panjabi MM (1990) Clinical biomechanics of the spine, JB Lipincott, Philadelphia, pp 110
44. Yoganandan N, Pintar F, Butler J, et al (1989) Dynamic response of human cervical spine ligaments. Spine 14: 1102–1110
45. Yoganandan N, Kumaresan S, Pintar FA (2000) Geometric and mechanical properties of human cervical spine ligaments. J Biomech Eng 122:623–629
46. Yoganandan N, Cusick JF, Pintar FA, Rao RD (2001) Whiplash injury determination with conventional spine imaging and cryomicrotomy. Spine 26:2443–2448